1996

PDX-1 is required for pancreatic out-growth and differentiation of the rostral duodenum

Martin F. Offield
Liberty University, moffield@liberty.edu

Tom L. Jetton

Patricia A. Labosky

Michael Ray

Roland W. Stein

See next page for additional authors

Development 122, 983-995 (1996)
Printed in Great Britain © The Company of Biologists Limited 1996
DEV6194

PDX-1 is required for pancreatic outgrowth and differentiation of the rostral duodenum

Martin F. Offield[1], Tom L. Jetton[2], Patricia A. Labosky[1,3], Michael Ray[1], Roland W. Stein[2], Mark A. Magnuson[2], Brigid L. M. Hogan[1,3] and Christopher V. E. Wright[1,*]

[1]Department of Cell Biology, [2]Department of Molecular Physiology and Biophysics, [3]Howard Hughes Medical Institute, Vanderbilt University School of Medicine, 1161 21st Avenue South, Nashville, TN 37232-2175, USA

*Author for correspondence (e-mail: wrightc@ctrvax.vanderbilt.edu)

SUMMARY

It has been proposed that the *Xenopus* homeobox gene, *XlHbox8*, is involved in endodermal differentiation during pancreatic and duodenal development (Wright, C. V. E., Schnegelsberg, P. and De Robertis, E. M. (1988). *Development* 105, 787-794). To test this hypothesis directly, gene targeting was used to make two different null mutations in the mouse *XlHbox8* homolog, *pdx-1*. In the first, the second *pdx-1* exon, including the homeobox, was replaced by a neomycin resistance cassette. In the second, a *lacZ* reporter was fused in-frame with the N terminus of PDX-1, replacing most of the homeodomain. Neonatal *pdx-1*$^{-/-}$ mice are apancreatic, in confirmation of previous reports (Jonsson, J., Carlsson, L., Edlund, T. and Edlund, H. (1994). *Nature* 371, 606-609). However, the pancreatic buds do form in homozygous mutants, and the dorsal bud undergoes limited proliferation and outgrowth to form a small, irregularly branched, ductular tree. This outgrowth does not contain insulin or amylase-positive cells, but glucagon-expressing cells are found. The rostral duodenum shows a local absence of the normal columnar epithelial lining, villi, and Brunner's glands, which are replaced by a GLUT2-positive cuboidal epithelium resembling the bile duct lining. Just distal of the abnormal epithelium, the numbers of enteroendocrine cells in the villi are greatly reduced. The PDX-1/β-galactosidase fusion allele is expressed in pancreatic and duodenal cells in the absence of functional PDX-1, with expression continuing into perinatal stages with similar boundaries and expression levels. These results offer additional insight into the role of *pdx-1* in the determination and differentiation of the posterior foregut, particularly regarding the proliferation and differentiation of the pancreatic progenitors.

Key words: gene targeting, PDX-1, IDX-1, STF-1, IPF-1, XlHbox8, pancreas, duodenum

INTRODUCTION

While the Hox cluster homeobox genes play critical roles in pattern formation along the main body and limb axes during early embryogenesis (for review see Krumlauf, 1994; McGinnis, 1994), several homeobox genes outside these clusters are required for the development of specific organs. Mutations in *pit-1*, which is expressed in the developing pituitary, lead either to reduction in pituitary function or to loss of the pituitary gland (Camper et al., 1990; Li et al., 1990). Similarly, inactivation of *Hox11*, which is expressed – among other places – in the mesodermal precursors of the spleen, produces asplenia in homozygous mutant mice (Roberts et al., 1994).

Based on its expression pattern, we hypothesized that the *Xenopus* homeobox gene *XlHbox8* plays a key role in regionalization of the posterior foregut, specifically in pancreatic and duodenal development (Wright et al., 1988). Mammalian homologs of *XlHbox8* were recently cloned as putative regulators of insulin and somatostatin gene transcription. In mouse, the protein product was called IPF-1 (insulin promoter factor-1; Ohlsson et al., 1993), and in rat, either STF-1 (somatostatin transcription factor-1; Leonard et al., 1993), or IDX-1 (islet-duodenum homeobox gene-1; Miller et al., 1994). The gene has recently been renamed *pdx-1* (for *p*ancreatic and *d*uodenal homeobo*x* gene-*1*) by the International Committee on Standardized Genetic Nomenclature for Mice, a name based on: (1) the developmentally restricted expression within the pancreas and duodenum and (2) the mutant phenotype of these tissues in animals that are homozygous null at the locus, as described here.

Mouse and frog PDX-1 share 100% identity in the homeodomain and 67% similarity in the N-terminal domain, and are expressed very comparably during embryogenesis (Peshavaria et al., 1994; Guz et al., 1995; Wright et al., 1988; Miller et al., 1994; Ohlsson et al., 1993; Leonard et al., 1993). In mouse embryos, PDX-1 expression precedes insulin and glucagon expression, and is first detected at 8.5 dpc in the dorsal endoderm of the gut while it is still an open tube. At 9.5 dpc, PDX-1 expression marks the dorsal and ventral pancreatic buds and the duodenal endoderm between them (Guz et al., 1995). In the adult, PDX-1 expression is maintained in the duodenal epithelium (Guz et al., 1995; Miller et al., 1994), and in the insulin-secreting islet β-cells, where it may trans-

activate the insulin gene (Peshavaria et al., 1994; Ohlsson et al., 1993; Peers et al., 1994; our unpublished observations).

We report here the use of gene targeting to study the role of *pdx-1* in endodermal development. Two different targeting experiments were performed, both of which are expected to generate null mutations, but the second experiment inserted a β-galactosidase (β-gal) reporter cassette into the locus, allowing the detection of endodermal cells normally expressing *pdx-1* in the presence and absence of functional PDX-1 protein. While our targeting experiments were in progress, Jonsson et al. (1994) reported that *pdx-1*$^{-/-}$ pups are apancreatic and die postnatally with a highly elevated urine glucose level. Consistent with this, both of our mutations also result in apancreatic mice. However, we find that pancreatic buds form in homozygous null mutants, but that they undergo only limited ductal outgrowth and branching, with a blockage of pancreatic endocrine and exocrine differentiation. In addition, malformations localized to the rostral duodenum occur in *pdx-1*$^{-/-}$ animals, often preventing gastric emptying, and the numbers of enteroendocrine cells in this region are reduced. These data are discussed in terms of a role for *pdx-1* in posterior foregut determination, specifically in the differentiation of the pancreas and rostral duodenum.

MATERIALS AND METHODS

Gene targeting constructs

Murine *pdx-1* genomic clones were isolated from a 129/Sv strain library using a 500 bp *Mlu*I-*Bam*HI fragment of a rat STF-1 cDNA (gift from Mark Montminy, Salk Institute) and *pdx-1* cDNAs isolated in this laboratory. All fragments, constructs and probes described here derive from one λ clone containing the entire *pdx-1* locus (see Fig. 1A). Gene targeting constructs were produced in pKO-I (gift from Manfred Blessing), which contains PGK-II and MC1 thymidine kinase (tk) cassettes flanking an MC1neo^r cassette, and unique *Xho*I and *Bam*HI sites on the PGK-IItk and MC1tk sides of the neo^r cassette, respectively.

The XBko construct contains a 7 kb *XbaI/BamHI* 5′ arm of homology inserted into the *Xho*I site and a 1.5 kb *Pst*I/*Xba*I 3′ arm inserted into the *Bam*HI site. The PDX-1/β-gal targeting construct, designated XSlacZ, has the same 3′ arm as XBko, but the 5′ homology extends from an *Xba*I site to a *Sma*I site in exon 2 (Fig. 1A), and is fused in-frame to a β-gal cassette from pPD1.27 lacZ, which encodes bacterial β-gal with SV-40 nuclear localization and polyadenylation signals (Fire et al., 1990). Fidelity of XBko and XSlacZ plasmid construction and reading frame maintenance were confirmed by extensive sequencing and restriction mapping. Constructs were released from the vector by *Not*I digestion prior to electroporation. The alleles resulting from homologous recombination of XBko and XSlacZ are designated *pdx*^{tm1CVW} and *pdx*^{tm2CVW}, respectively, according to the guidelines of the International Committee on Standardized Genetic Nomenclature for Mice (Jackson Labs). For clarity, we refer to these mutant alleles herein as pdx^{XBko} (XBko) and pdx^{lacZko} (XSlacZ).

Electroporation and selection of ES cell clones

For each targeting construct, 4×10^7 ES cells (129 strain-derived line R1; kind gift from Drs Janet Rossant and Andras Nagy) were electroporated with 200 μg of the linearized targeting construct in 0.8 ml phosphate-buffered saline (PBS) with one pulse of 800 V/3 μF from a Gene Pulser (Biorad). ES cells were then subjected to positive-negative selection with geneticin (GIBCO) and gancyclovir (Syntex) according to standard protocols (Hogan et al., 1994; Winnier et al., 1995). After

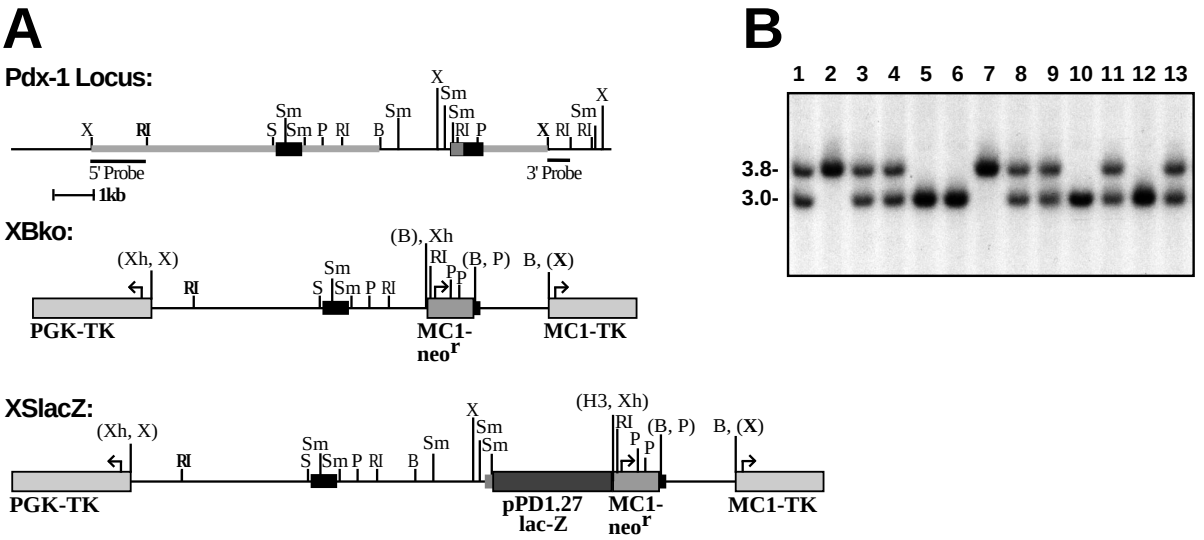

Fig. 1. Targeted mutagenesis of *pdx-1*. (A) *pdx-1* contains two exons; the second exon contains the homeodomain coding sequence (lighter box). Targeted deletions of homeobox sequences were produced with the XBko construct, which replaces intron and protein coding sequences of the second exon with a MC1neo^r cassette, and the XSlacZ construct, which fuses a nuclear targeted β-galactosidase cassette (with its own 3′ SV-40 poly(A) signals followed by the MC1neo^r cassette driven by its own promoter) in frame with PDX-1. The XBko construct contains 7 kb of 5′ homology and 1.5 kb of 3′ homology (thickened lines on the *pdx-1* locus map). The XSlacZ construct contains 9 kb of 5′ homology, from the 5′ *Xba*I site to the *Sma*I site in the homeobox, and the same 3′ region of homology as XBko. Both constructs contain 5′ PGK-II thymidine kinase and 3′ MC1-thymidine kinase cassettes (transcription direction for tk and neo^r cassettes is indicated by arrows). Homologous recombinants were detected using the 3′ probe (500 bp *Xba*I-*Eco*RI fragment) on Southern blots of *Eco*RI digested DNA by an 800 bp shift from 3 kb (endogenous locus) to 3.8 kb (targeted locus). Further Southern blot analysis of targeted lines used *Eco*RI, *Pst*I, and *Xba*I digested DNA probed with both the 3′ probe and 5′ probe (2 kb *Xba*I-*Eco*RI, internal probe). (B) Southern analysis of DNA samples from a complete litter of pdx^{XBko} pups (derived from +/– mating) digested with *Eco*RI and probed with the 3′ probe. X, *Xba*I; RI, *Eco*RI; S, *Sac*I; Sm, *Sma*I; P, *Pst*I; B, *Bam*HI.

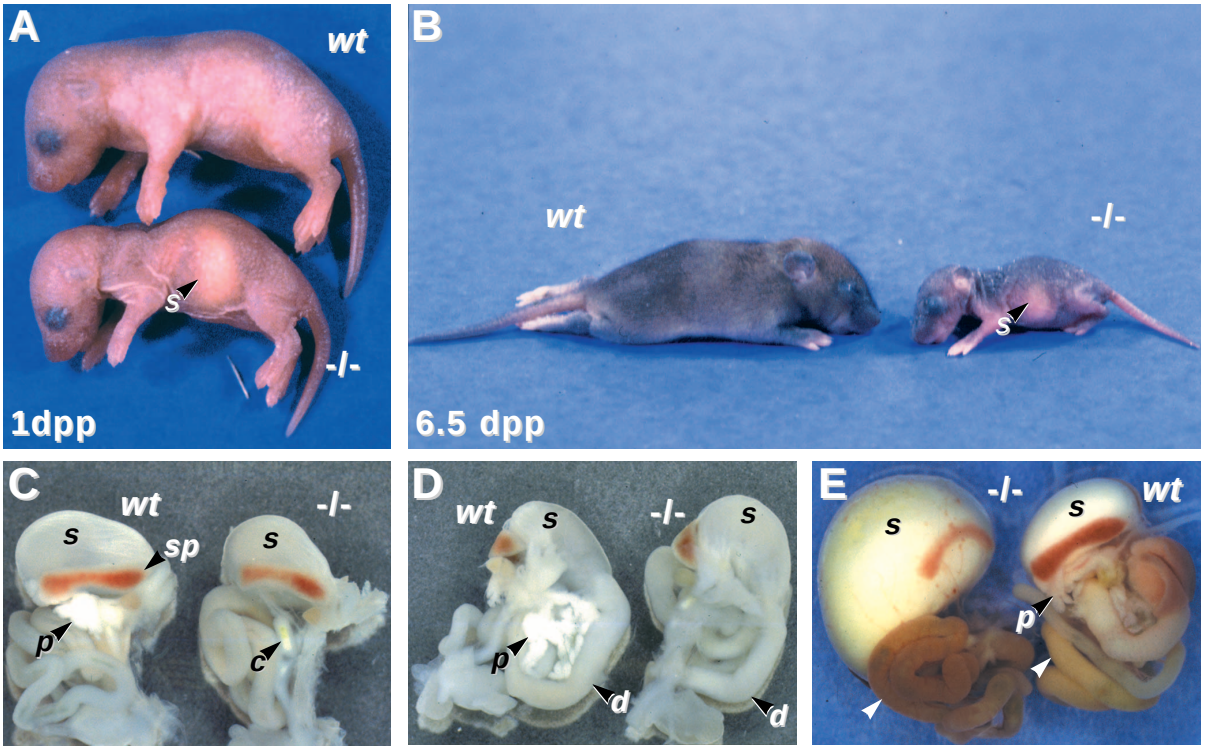

Fig. 2. Gross analysis of pdx^{XBko} animals. (A) At 1 day post-partum (1 dpp), the pdx$^{XBko-/-}$ pups (bottom) begin to show signs of growth retardation and apparent dehydration, compared to wild-type littermates (top). (B) By 6.5 dpp, *pdx-1*$^{-/-}$ animals are extremely dehydrated. Though their stomachs contain milk (arrowhead), they show approx. 60% reduction in weight compared to wild-type littermates. (C,D) 18.5 dpc$^{-/-}$ embryos (right) show a complete absence of pancreatic tissues and malformations at the stomach/duodenal junction (see Fig. 3 for these malformations). (E) In many 1 dpp$^{-/-}$ pups (left), a stomach/duodenal obstruction occurs, as evidenced by stomach distension and a lack of gastric emptying. The small intestines appear to be empty (white arrowheads; note the light-colored wild-type gut, indicating milky gut contents). s, stomach; p, pancreas; d, duodenum; sp, spleen; c, colon.

7-10 days, individual clones (700 for XBko, and 500 for XSlacZ) were isolated and DNA screened for the presence of the targeted allele.

DNA analysis

DNA from doubly resistant ES cell clones was prepared as previously described (Hogan et al., 1994), and samples were screened by *Eco*RI digestion and Southern blot hybridization with the 3′ external probe (Fig. 1A). Cultures of targeted lines were expanded from which DNA was analyzed by Southern blot analysis of *Xba*I, *Eco*RI, and *Pst*I digests with the 3′ probe, and internal 5′ probe (Fig. 1A). Pups and embryos were genotyped by Southern blot analysis using *Eco*RI digestion and the 3′ probe. DNA from pups was obtained from tail snips at 3 weeks of age. For 18.5 dpc embryos, the cerebellum or a piece of liver was used to obtain DNA. For younger embryos, the extraembryonic membranes and/or the entire brain were used, depending on the age of the embryo. DNA was prepared as described (Hogan et al., 1994), and analyzed with the 3′ probe.

Generation of chimeric mice

ES cells were injected into C57BL/6 blastocysts that were transferred into pseudopregnant ICR females as described by Hogan et al. (1994). Male chimeras were bred to Black Swiss females (Taconic Farms) and agouti offspring were genotyped by Southern blot analysis. Heterozygous (Black Swiss × 129) offspring were interbred to produce homozygous animals.

X-gal staining

pdx^{lacZko} embryos and tissues were dissected in PBS and kept on ice until fixation. Embryos younger than 12 dpc were stained whole. For older embryos, the entire alimentary tract was dissected out. Fixation and staining were as previously described (Bonnerot and Nicolas, 1993). Briefly, tissues were fixed in 4% paraformaldehyde at 4°C with agitation for 30-40 minutes, permeabilized (except for 9.5 dpc embryos, which were simply rinsed in PBS), and X-gal stained overnight at room temperature. Tissues were post-fixed in 4% paraformaldehyde at 4°C and then rinsed in PBS. Some tissues were cleared for photography by two 15 minute incubations in 100% methanol followed by 2:1 benzyl benzoate:benzyl alcohol. Afterwards, these were rinsed twice with methanol before transfer to 100% ethanol prior to paraffin embedding. X-gal staining patterns are specific for *pdx-1* driven β-gal activity, because homozygous wild-type embryos were devoid of background staining at the stages analyzed.

Immunohistochemistry

Paraffin or cryostat sections (5 μm) were hydrated to PBS and subjected to either immunoperoxidase or immunofluorescence staining. Immunoperoxidase staining was carried out as previously described (Jetton et al., 1994). Primary antibodies to the following antigens (made in rabbit unless otherwise indicated) were used at the indicated dilutions: insulin (Zymed), prediluted; mouse monoclonal to human insulin (Zymed), prediluted; guinea pig anti-insulin (Linco), 1:1000; guinea pig anti-insulin C-peptide (Linco), 1:1000; amylase (gift from R. MacDonald and G. Swift, Dallas), 1:1000; mouse GLUT2 (gift from B. Thorens, Lausanne), 1:2000; glucagon (Linco), 1:1000; pancreatic polypeptide (PP; ICN), 1:1000; somatostatin (ICN), 1:1000; neuron-specific enolase (NSE; Zymed), prediluted;

chromagranin A (Zymed), prediluted; glucagon-like peptide-1 (GLP-1; Peninsula), 1:1000; gastric inhibitory peptide (GIP; Peninsula), 1:1000; secretin (Peninsula), 1:1000; cholecystokinin (CCK; Peninsula), 1:2000; serotonin (Zymed), prediluted. Primary antibodies were incubated overnight at room temperature or 4°C. For immunoperoxidase detection, goat anti-rabbit-horseradish peroxidase (HRP) antibody (Jackson Immunoresearch; 1:500) or donkey anti-mouse-biotin IgG (Jackson Immunoresearch; 1:500) followed by Z-Avidin-HRP (Zymed Laboratories; 1:500) were incubated for 1 hour at 22°C. Immunoperoxidase was detected with DAB/H_2O_2 for 2-5 minutes followed by counterstaining with hematoxylin. For immunofluorescent studies the following secondary antibodies (Jackson Immunoresearch; 'ML grade') were used: donkey anti-rabbit-FITC, 1:250; donkey anti-rabbit-Cy3 at 1:1000; donkey anti-guinea pig-FITC, 1:250; and donkey anti-guinea pig-Cy3, 1:1000. Some samples were counterstained with the nuclear dye, YO-PRO-1 (Molecular Probes; 1:10,000 dilution in PBS).

Fluorescently labeled samples were imaged on a Zeiss LSM 410 confocal microscope. Excitation wavelengths were 488 nm from an Ar-Kr laser (for YO-PRO-1 or FITC) and 543 nm from a HeNe laser (for Cy3). Fluorescence images were ascribed green (YO-PRO-1 and FITC) or red pseudocolors (Cy3), and were digitally optimized using the Zeiss system software (v.3.56b). TIFF images (512 × 512 pixel) were transferred to either a Silicon Graphics Indigo imaging workstation or a Macintosh PowerMac 8100 for secondary optimization and formatting, and printed on a Tektronix dye sublimation printer.

Periodic acid-Schiff staining

Sections were hydrated to tap water, oxidized in 0.5% periodic acid (w/v) for 10 minutes, washed for 5 minutes, rinsed briefly in demineralized water and stained in Schiff's reagent (Fisher) for 10 minutes. Following three rinses in 9.5% sodium metabisulfite (w/v), sections were washed and counterstained with Harris's hematoxylin (Sigma Chemical).

RESULTS

Targeted mutagenesis of *pdx-1*

Two different targeting constructs were used to disrupt *pdx-1* (see Fig. 1A). In the XBko construct, the protein-coding sequences in exon 2 are deleted, including those encoding the DNA-binding homeodomain. In XSlacZ, nuclearly targeted β-gal is fused in-frame with PDX-1 at the 5′ end of exon 2, deleting the homeodomain and bringing β-gal activity under the control of *pdx-1* promoter/enhancer elements. Positive-negative selection was carried out, and doubly resistant ES cell clones were screened by Southern blot analysis, which confirmed precise targeting for both XBko and XSlacZ without rearrangement, duplications, or additional random insertions (Fig. 1A,B; data from 5′ probe not shown). The targeting frequency was 1 in 34 of doubly resistant clones for XBko (13 lines), and 1 in 43 (7 lines) for XSlacZ.

Chimeras were produced from 3 lines for pdx^{XBko} (lines BA5, CB8, and CC4), and 4 lines for pdx^{lacZko} (3D2, 3D4, 2E3, and 2G2). Germline transmission was obtained for all seven lines, and breeding to Black Swiss mice generated heterozygotes. No reduction in the viability or fertility of *pdx-1* heterozygous mice was detected, and male and female heterozygotes were bred to produce homozygous mutant animals for each allele. Pups of genotype *pdx-1* +/+, +/– and –/– are born in the Mendelian distribution of 1:2:1 (e.g. Fig. 1B). For pdx^{XBko} the ratio (percentage of total) was 23:50:27 (n=230), and for pdx^{lacZko} it was 27:47:27 (n=60); thus no embryo loss in utero is caused by the mutation. The homozygous null mutant phenotype is indistinguishable between animals derived from both targeted alleles, and data from a detailed analysis of CC4 and BA5 (pdx^{XBko}), and 2E3 and 3D4 (pdx^{lacZko}) are reported here.

The homeodomain helix-turn-helix motif provides a sequence-specific DNA recognition function (see Gehring et al., 1994). While certain *Drosophila* homeodomain proteins have some function without their homeodomains (Fitzpatrick et al., 1992), and the production of mammalian Hox gene mRNAs lacking the homeobox has been reported (e.g. Murphy and Hill, 1991), we expect that the abolition of DNA-binding activity in both of our targeted mutations generates functional null alleles of *pdx-1*. That the pdx^{XBko} and $pdx^{lacZko-/-}$ mutants represent null alleles is supported by the following: (1) PDX-1 was not detected in 9.5 dpc –/– embryos (pdx^{XBko}) by immunostaining with antibodies against the N-terminus of PDX-1 (data not shown), and (2) there was no dominant negative effect in $pdx^{XBko+/-}$ or $pdx^{lacZko+/-}$ animals.

Gross analysis of homozygous *pdx-1* mutants

Immediately after birth, pdx^{XBko} and $pdx^{lacZko-/-}$ null mutants are indistinguishable from +/+ or +/– littermates. However, within the first day postpartum (dpp), –/– animals show signs of growth retardation and dehydration, although they feed because their stomachs contain milk (Fig. 2A). By 1 dpp, the stomachs of some –/– mutants are distended because of a lack of gastric emptying into the gut (Fig. 2E), which may result from malformations at the stomach-duodenum junction that are described below. $Pdx^{XBko-/-}$ pups can survive until at least 6.5 dpp (Fig. 2B), but the animals were not maintained longer for ethical reasons. At this age, $pdx^{XBko-/-}$ pups still have milk in their stomachs, but they are severely dehydrated, having a thin and cracking skin with very little fur, and are much smaller (up to 60% less by weight) than +/+ or +/– littermates. The developmental retardation in –/– pups is likely attributable to malnutrition resulting from lack of digestion in the absence of a pancreas and functional rostral duodenum (see below), and/or diabetic consequences of the loss of pancreas (Jonsson et al., 1994). Heterozygotes are healthy and otherwise indistinguishable from +/+ littermates at the level of examination described here. However, because PDX-1 may be an insulin gene activator (see Introduction), physiological defects under certain feeding conditions in heterozygous $pdx\text{-}1^{+/-}$ animals cannot yet be ruled out.

Dissection of $pdx^{XBko-/-}$ pups at 1 dpp revealed that the liver, gall bladder, spleen, stomach, common bile duct, and other viscera are present and normal, but that the pancreas is noticeably absent in all cases (Fig. 2C,D). This observation is entirely consistent with the conclusion of Jonsson et al. (1994) that a similar null mutation of *pdx-1* blocked pancreatic development.

β-gal expression in pdx^{lacZko} heterozygotes detects *pdx-1* expression

In $pdx^{lacZko+/-}$ animals analyzed between the ages of 9.5 dpc and adult (n=35), *pdx-1* expression, as visualized by X-gal staining, marks endodermal tissues previously shown to express *pdx-1* endogenously (Guz et al., 1995; Miller et al., 1994; Ohlsson et al., 1993), while +/+ embryos remained completely unstained. Thus, the PDX-1/β-gal fusion protein

expression provides a sensitive way of tracing cells expressing *pdx-1*, without alterations caused by the neo^r cassette located 3′ of the *lacZ* reporter (Fig. 1A).

In heterozygous 9.5 dpc embryos, PDX-1/β-gal is expressed throughout the dorsal and ventral pancreatic buds and in the intervening endoderm of the presumptive duodenum (Fig. 3A). At 11.5 dpc, expression continues in the dorsal and ventral buds, and the duodenal epithelium staining is more intense than earlier (Fig. 3B). In addition, the epithelia of the cystic duct, common bile duct, and antral stomach are stained at 11.5 dpc (Fig. 3B). We conclude that this reporter gene approach provides a more complete understanding of the tissues expressing PDX-1 than previous analyses of the endogenous antigen, which is unusually sensitive to the fixation conditions (our unpublished observations). The PDX-1/β-gal expression boundaries at the liver/common bile duct and at the antral/fundic stomach boundary are relatively sharp, while expression in the duodenum declines caudally, becoming increasingly punctate in the more distal gut (Fig. 3B).

At 16.5 dpc, PDX-1/β-gal expression is maintained in the antral stomach, common bile duct and cystic duct, and in duodenal enterocytes and enteroendocrine cells (Fig. 3C,D; data not shown). The biliary ducts proximal to the common bile duct also express PDX-1/β-gal (data not shown). At this stage, the embryonic gut has changed from a pseudostratified to a columnar epithelium, the pancreatic buds have fused, and differentiation of exocrine and endocrine cell types has started. Pancreatic PDX-1/β-gal staining begins to be extinguished in non-islet cell types at this stage (see below). Towards the caudal limit of the expression domain of *pdx-1* in the gut mucosa, X-gal-positive cells are few in number and well dispersed, and colocalization of the *pdx-1* expression with enteroendocrine peptide markers is very often encountered (data not shown). Just before birth (18.5 dpc), pancreatic PDX-1/β-gal expression becomes restricted mostly to the developing islets. In the gut, enterocytes and enteroendocrine cells of the rostral duodenum epithelium are all labeled, and scattered epithelial cells again stain in the more distal gut (data not shown). At all stages examined, X-gal staining is absent from mesodermal tissues (see below).

PDX-1/β-gal expression is maintained in homozygous null animals

As summarized in Fig. 3, an analysis of embryos from 9.5-16.5 dpc (n=18) shows that the intensity and anteroposterior extent of PDX-1/β-gal expression in pdx^{lacZko} homozygous null animals is similar to that in pdx^{lacZko} heterozygotes. This includes conspicuous labeling of the early dorsal and ventral pancreatic buds, which are comparable to those in +/– littermates (compare Fig. 3A,E), and the endodermal lining of the prospective duodenum (Fig. 3E,F). At 11.5 and 16.5 dpc, the expression boundaries at the liver and within the stomach are the same in +/– and –/– littermates (Fig. 3F-H). We conclude that PDX-1 is not necessary for maintaining its own expression, nor for the survival of most endodermal cells that normally express it, although at this level of analysis the loss of a relatively low number of scattered cells cannot be ruled out. Most notably, the generation of the pancreatic buds does not require *pdx-1* function.

Loss of PDX-1 function blocks pancreatic bud outgrowth

At 11.5 dpc, a separate outgrowth derived from the ventral pancreatic bud is no longer visible in pdx$^{lacZko-/-}$ embryos (Fig. 3F), possibly because the cells derived from the ventral bud became incorporated into the biliary duct, or died. The common bile duct is greatly shortened, and the liver primordium is juxtaposed to the duodenum (Fig. 3F). The extensive dorsal pancreatic outgrowth of normal +/+ or +/– embryos (Fig. 3B-D) is replaced by a short ductular structure in pdx$^{lacZko\ -/-}$ animals (e.g. Figs 3F, 4). A ‘duodenal’ gut tube is seen in mutant embryos, and it is of similar length to that in wild-type embryos, as judged by the domain of PDX-1/β-gal expression (e.g. Fig. 3F,G). At any stage examined, homozygous null mutant embryos for either mutant allele never displayed necrotic plaques that might indicate large areas of cell death caused by the absence of PDX-1 function.

The dorsal ductule derived from the dorsal bud in –/– animals persists into perinatal stages and goes through some outgrowth and irregular branching (Fig. 4), although it is stunted greatly compared to the dorsal pancreas of pdx$^{lacZko+/-}$ embryos (e.g. compare Fig. 3C with 3G, and Fig. 4A with 4B,C,D). Similarly abrogated ductular trees were noted in all –/– mutant embryos (from 11.5-18.5 dpc) in both pdx^{XBko} (Fig. 4D) and pdx^{lacZko} (Fig. 4B,C) animals. Such ductal structures, other than the normal pancreatic and biliary ducts, are never present in +/+ or +/– embryos.

Pancreatic marker expression in *pdx-1* $^{-/-}$ mutant embryos

We next determined whether any cells present in or around the dorsal ductule of *pdx-1*$^{-/-}$ embryos express markers of specific mature pancreatic cell types. As reported previously (Pang et al., 1994; Teitelman et al., 1993), glucagon-positive cells are found in +/– 9.5 dpc embryos as small clusters peripheral to, and dispersed within, the pancreatic bud (Fig. 5A). Similar populations of glucagon-positive cells are found in the pancreatic buds of –/– embryos (Fig. 5B). In both +/– and –/– pancreatic buds, the peripheral glucagon-positive cells do not express *pdx-1*, as indicated by absence of PDX-1/β-gal expression, but the *pdx-1* expression status of glucagon-positive cells within the bud is somewhat uncertain because of masking by intensely X-gal-positive cells.

In 11.5 dpc pdx^{lacZko} heterozygotes, glucagon-positive cells are again detected within the pancreatic buds, and in clusters of X-gal negative cells at the bud periphery (Fig. 5C). In pdx$^{lacZko-/-}$ mutant embryos at the same stage, a small number of glucagon-positive cells is found at, or close to, the junction of the dorsal ductule with the gut lumen (data not shown), but glucagon-positive cells are absent from distal regions of the dorsal ductule (Fig. 5D).

At 16.5 dpc and later, pdx^{lacZko} heterozygotes show large numbers of glucagon- and insulin-positive cells in the emerging islets (Fig. 5E,G), and amylase expression in the developing exocrine acini (Fig. 5F). In 16.5 dpc pdx^{lacZko} homozygous null embryos (n=3), PDX-1/β-gal negative, glucagon-positive, cells are detected within the dorsal ductule (e.g. Fig. 5I), but amylase is still not detectable (compare Fig. 5F with J). In light of the role proposed for *pdx-1* in the derivation of mature β cells in the pancreatic islet (Guz et al., 1995),

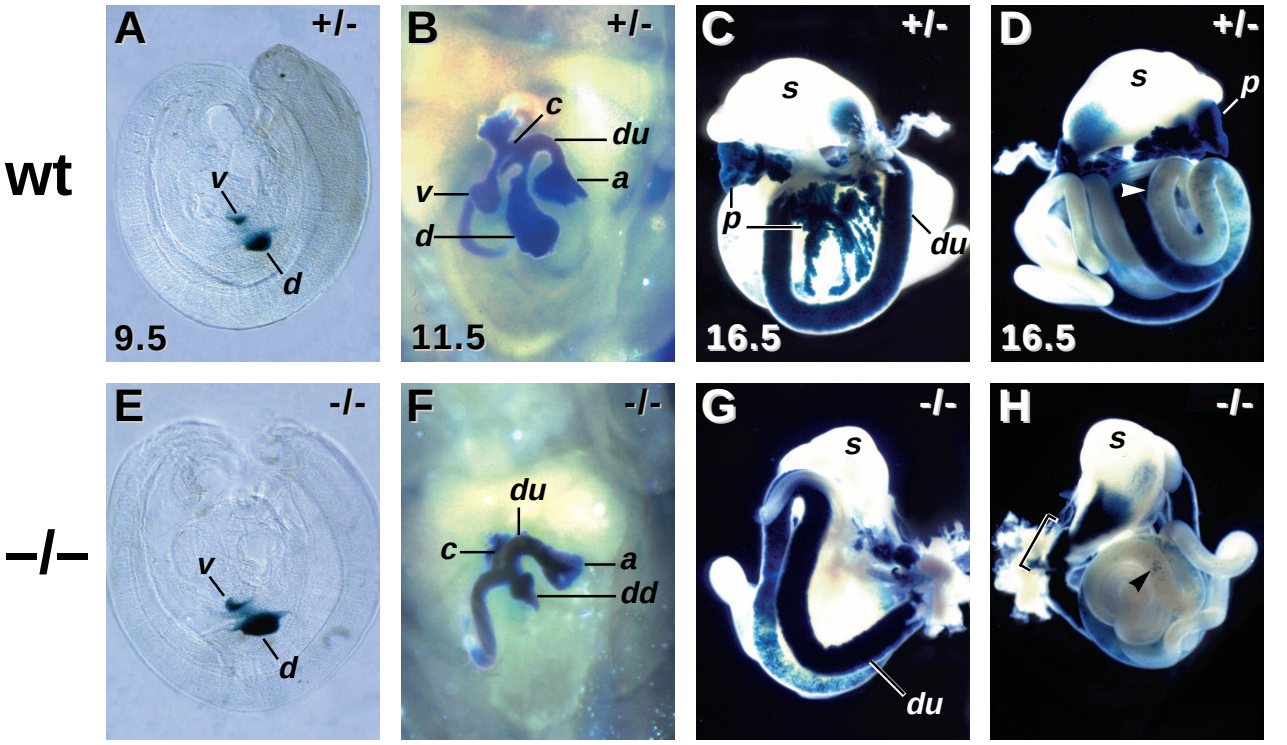

Fig. 3. Tracking of *pdx-1* expressing tissues in pdx^{lacZko} embryos. (A,E) At 9.5 dpc, dorsal and ventral buds stain for β-galactosidase (β-gal) expression in both pdx$^{lacZko+/–}$ and –/– embryos. The presumptive duodenum between the buds is also stained. The heads were removed to obtain DNA for genotyping; anterior is upper right. (B,F) The ventral (v) and dorsal (d) buds are much larger by 11.5 dpc in wild-type +/– animals and stain throughout with X-gal. However, pancreatic buds are absent in –/– littermates. An extra duct structure (dd) replaces the dorsal bud. X-gal staining labels the antral stomach (a), duodenum (du), and common bile duct (c) in both +/– and –/– embryos. (C,G) At 16.5 dpc, a similar staining pattern in seen in both wild-type +/– and –/–. Pancreatic tissues are still undetected in –/– embryos. (D,H) In both +/– and –/– embryos, staining in the gut epithelium tapers off gradually from the distal duodenum to the ileum (arrowheads indicate punctate staining in the presumptive jejunum). The bracket in H indicates the region corresponding to the cuboidally lined discontinuity at the stomach/duodenal junction. v, ventral bud; d, dorsal bud; c, common bile duct; dd, dorsal ductule; du, duodenum; a, antral stomach; s, stomach; p, pancreas.

we searched extensively for insulin-expressing cells in homozygous null mutants, under conditions in which wild-type sibling tissues displayed large numbers of insulin-positive cells (Fig. 5G,H). No insulin-positive cells were detected by immunohistochemical analysis of the entire serially sectioned dorsal ductule and rostral duodenum, in a total of three embryos at 16.5 dpc (Fig. 5K), or five embryos at 18.5 dpc (Fig. 5L).

To further characterize the dorsal ductule, we used immunohistochemistry to examine the expression of glucose transporter-2 (GLUT2; Thorens et al., 1990), while also double-staining for insulin or glucagon. In wild-type embryos, the GLUT2 signal is intense in the common bile duct epithelium (Fig. 6A) and, as in rat (Thorens et al., 1990), is expressed at lower levels in the basolateral surfaces of the

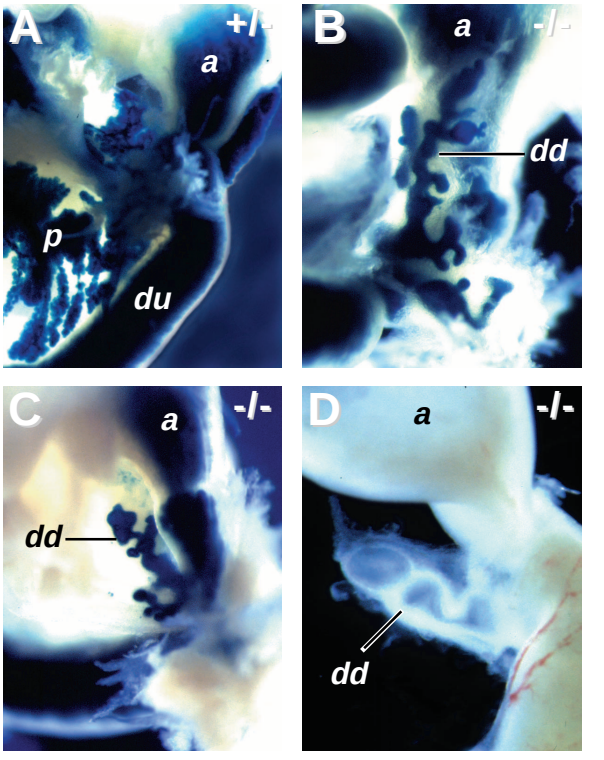

Fig. 4. Aberrant pancreatic duct structures in *pdx-1*$^{–/–}$ embryos. (A) At 16.5 dpc, a regular branching pattern is seen in the pancreas of +/– embryos. (B and C) In –/– mutant littermates, the pancreatic tissues are replaced by small irregularly branched dorsal ductules (dd) lined by a PDX-1/β-gal-expressing epithelium. These vary somewhat in size and complexity but are seen in all –/– animals (*n*=24). (D) Similar dorsal ductules are produced in pdx^{XBko} embryos (*n*=61), shown here at 18.5 dpc. du, duodenum; a, antral stomach; s, stomach; p, pancreas; dd, dorsal ductule.

columnar epithelial cells of the duodenal villi (Fig. 6B,D). GLUT2 is also expressed at relatively high levels in the early pancreatic buds (Pang et al., 1994), but is then downregulated so that only very low levels exist in the pancreatic duct epithelium of late gestation embryos (data not shown; Bob Gimlich, Genetics Institute, personal communication). In contrast, the epithelium of the dorsal ductule in *pdx-1*$^{-/-}$ mutants expresses GLUT2 intensely (Fig. 6C), with several evaginations showing somewhat decreased GLUT2 signal intensity. Many of these evaginations have small clusters of glucagon-positive cells at their distal tips (Fig. 6C,E,F), in addition to glucagon-positive cells within the dorsal ductule epithelium itself (Fig. 5I).

Based on the morphology of the dorsal ductule and the absence of expression for specific markers, we conclude that differentiation of islets, mature pancreatic β cells, and acinar cells is blocked in *pdx-1*$^{-/-}$ embryos, in agreement with the findings of Jonsson et al. (1994). Non-epithelial and epithelial

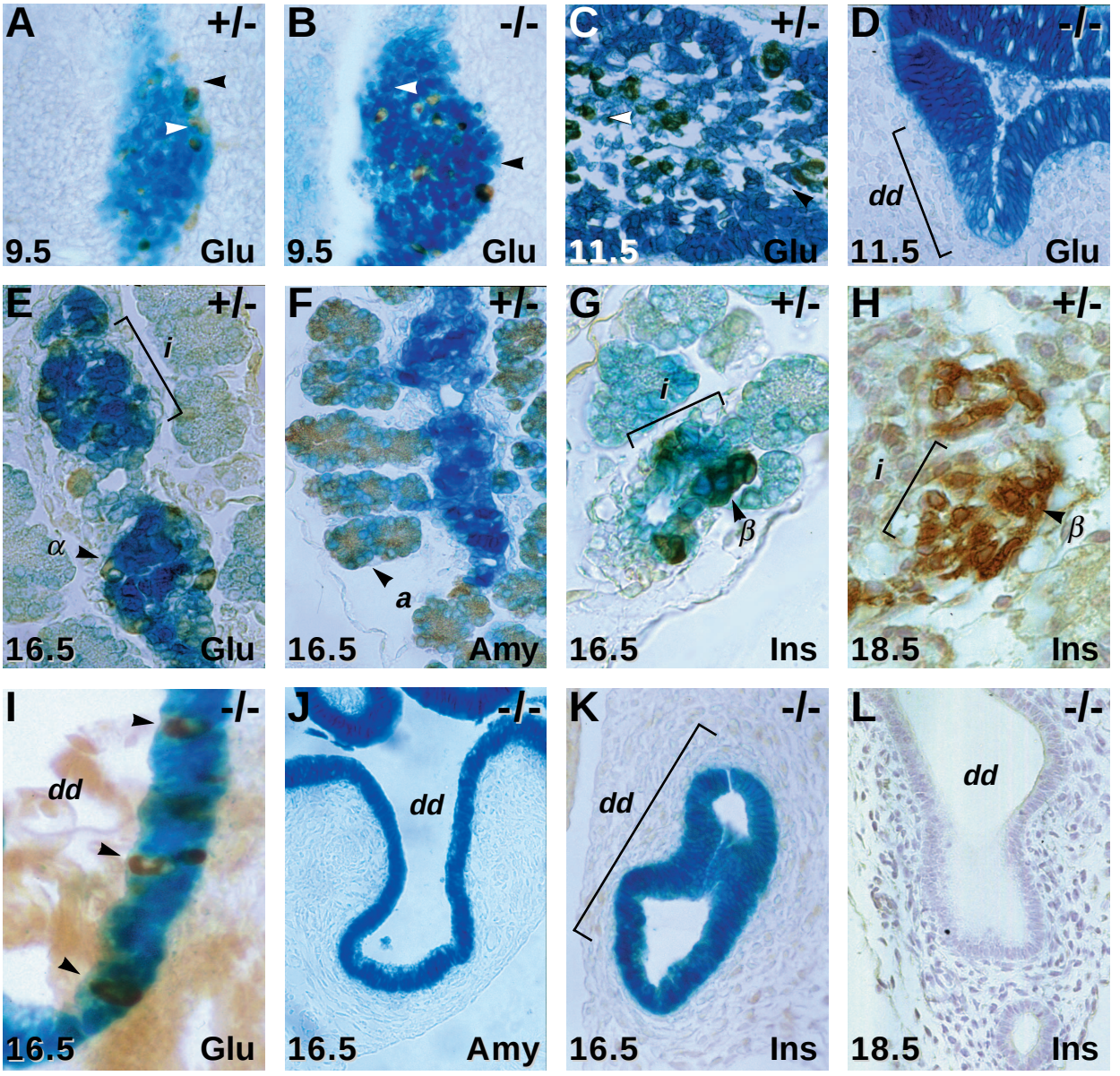

Fig. 5. Pancreatic marker expression in pdx^{XBko} and pdx^{lacZko} embryos. (A,B) At 9.5 dpc in pdx$^{lacZko-/-}$ and +/– embryos, brown glucagon-positive cells are found in clusters (black arrowheads) at the endoderm/mesenchyme boundary and within the X-gal stained buds (white arrowheads). (C) At 11.5 dpc, wild-type pdx$^{lacZko+/-}$ embryos contain larger numbers of glucagon-expressing cells. (D) In 11.5 dpc –/– littermates, the dorsal pancreatic bud is replaced by the dorsal ductule (dd). Glucagon-expressing cells are not detected in distal regions of this ductule, but are found in epithelial tissue that is closer to the duodenal lumen (data not shown). (E) In 16.5 dpc pdx$^{lacZko+/-}$ embryos, glucagon-positive cells (α) are seen in the budding islets. (I) In –/– littermates, glucagon-positive cells (arrowheads) are seen within the X-gal stained epithelium of the ductules (dd). (F,J) Amylase is also detected at this stage in pdx$^{lacZko+/-}$ embryos in the acini (a), but is not seen in –/– animals. (G,H) A high level of insulin expression is seen at 16.5 and 18.5 dpc, respectively, in the developing islets of wild-type pdx$^{lacZko+/-}$ embryos, but is not detected at either time point (K,L) in the dorsal ductule or the malformed rostral duodenum in pdx$^{lacZko-/-}$ littermates. H,L were hematoxylin counterstained, but not X-gal stained. dd, dorsal ductule; i, islet; β, beta cell; a, acini; α, alpha cell.

glucagon-positive cells are found, but they are intimately associated with a GLUT2-positive dorsal ductule epithelium, and we therefore hypothesize that they are more like early embryonic glucagon-positive cells than mature islet cell types (see Discussion).

Malformations at the stomach/duodenum junction of *pdx-1*$^{-/-}$ null mutants

During the analysis of the defects in pancreatic development, we noted structural abnormalities centered around the rostral duodenum of *pdx-1*$^{-/-}$ embryos that might explain the lack of gastric emptying and subsequent stomach distension (Fig. 2E). These defects are summarized in Fig. 7. In normal late gestation embryos, the pyloric sphincter lies at the stomach/duodenum junction, and villi covered by a columnar epithelium protrude into the gut lumen throughout the rostral duodenum (Fig. 7A,B). In *pdx-1*$^{-/-}$ animals, the pylorus is very contorted, although at least some of its tissues are recognizable, such as the characteristic smooth muscle bands (data not shown). Because the expression of PDX-1/β-gal extends over the antral stomach (Figs 3, 4), this could indicate a direct role for *pdx-1* in the differentiation of antral stomach tissues, although it is possible that the pylorus defects are a consequence of the adjacent gut tube malformations described below.

In *pdx-1*$^{-/-}$ animals, the villi of the rostral-most duodenum are replaced by an area of smooth cuboidal epithelium (Fig. 7C-F), continuous with the dorsal ductule epithelium, resembling the cystic/biliary duct epithelium both in its morphology and in its GLUT2 expression (compare Fig. 6A with 6C,D). Similar structural alterations are also seen in pdx^{lacZko} homozygous null embryos, and the cells in this abnormal epithelium express PDX-1/β-gal (data not shown). The topology of the gut lumen over this region is changed profoundly from a fairly straight tube in normal embryos to a diverticulated or spiraled tube, and parts of the lumen are tightly constricted compared to the wild-type duodenum. Of 6 pdx$^{XBko-/-}$ animals analyzed, three 18.5 dpc embryos and two 1 dpp pups showed this phenotype. The remaining 18.5 dpc –/– animal showed an almost normal connection of the pylorus and rostral duodenal lumen, but the columnar to cuboidal conversion of epithelium and absence of villi was obvious (Fig. 7E).

Absence of Brunner's glands in *pdx-1* $^{-/-}$ mutants

Brunner's glands are epithelially derived submucosal glands that secrete bicarbonate and mucin into the duodenal lumen via connecting ducts. In mouse, they are located in a collar around the neck of the duodenum adjacent to the stomach (Fig. 7A,B). A small number of circular structures with a superficial similarity to Brunner's glands were observed in some pdx$^{XBko-/-}$ gut sections (Fig. 8B,D). To characterize these structures, sections of pdx$^{XBko-/-}$ and +/+ littermates were stained with periodic acid/Schiff's reagent (PAS), which detects the basic mucins of the lumenal surface and perinuclear Golgi in Brunner's gland cells (Fig. 8A,C). The structures found in *pdx-1*$^{-/-}$ embryos have a morphology different from that of Brunner's glands and do not stain with PAS (Fig. 8B,D), and we therefore conclude that they are duodenal crypts, or possibly dysfunctional Brunner's glands. It remains to be seen whether *pdx-1* is directly involved in the differentiation of these glands, or if their failed development is secondary to the abnormal morphogenesis of the rostral duodenum in homozygous null embryos. However, we note that Brunner's gland development involves epithelial budding and differentiation, which is reminiscent of the processes of pancreatic outgrowth. Numerous clustered evaginations of the PDX-1/β-gal-positive epithelium were noted in the rostral-most duodenum of some 16.5 dpc pdx$^{lacZko-/-}$ embryos (data not shown). These evaginations were not seen in older –/– embryos, and it is possible that they represent a transient stage of abnormal Brunner's gland development. Nevertheless, the absence of mature Brunner's glands supports the hypothesis that loss of PDX-1 function affects duodenal differentiation as well as pancreatic development.

Decreased numbers of duodenal enteroendocrine cells in *pdx-1*$^{-/-}$ embryos

Interspersed among the mucosal enterocytes, the mammalian gut epithelium contains enteroendocrine cells that are characterized by their morphology and their secretion of specific peptide hormones (see Solcia et al., 1987 for review). The relative abundance of the different cell types varies regionally along the gut; thus, they are useful markers of gut patterning. We therefore analyzed wild-type +/+ and –/– tissues from 18.5 dpc embryos for the distribution and number of these cell types by immunohistochemistry with neuroendocrine peptide antibodies. Late gestation embryos were analyzed because enteroendocrine cells are detected properly only after the gut has changed from a pseudostratified to a columnar epithelium with villi (occurring in mice between 16 and 18 dpc) and because neuroendocrine peptide expression is upregulated after 17 dpc in preparation for feeding (Roth et al., 1991). Postnatal animals were not analyzed because of variable pathological effects on the gut epithelium likely stemming from the digestive problems in these animals (see, for example Fig. 7C).

Cells positive for most gut neuroendocrine peptides (see Materials and Methods) were detected in pdx$^{XBko-/-}$ and +/+ littermates, but only secretin, CCK, and serotonin-positive cells were numerous enough for statistical comparisons. In pdx$^{XBko+/+}$ embryos, CCK, secretin, and serotonin expressing cells are abundant in the rostral duodenum just below the pylorus, and their numbers decline sharply towards the distal duodenum (Figs 9, 10). A reduction of approximately 60% in the numbers of all three cell types occurs in the rostral duodenum of pdx$^{XBko-/-}$ embryos, while in the more distal duodenum their numbers approach normal (Figs 9 and 10).

The enterocyte population of the duodenum and distal gut in pdx$^{XBko-/-}$ mutants was analyzed by immunohistochemistry for L-FABP and I-FABP (liver and intestinal fatty acid binding proteins: Cohn et al., 1992; Sweetser et al., 1988). Neither marker is expressed in the abnormal cuboidal epithelium of the rostral duodenum (data not shown). Just distal of this region, where villi are present, the expression of both enterocyte markers is indistinguishable between wild-type and mutant animals (data not shown). Furthermore, no obvious histological abnormalities or morphological defects in other regions of the gut were noted (data not shown).

DISCUSSION

Jonsson et al. (1994) have previously reported that null

mutation of the *pdx-1* gene prevents pancreatic development and differentiation of exocrine cells and islet β cells, resulting in extreme hyperglycemia and perinatal death. The analysis presented here of two similar *pdx-1* mutant alleles corroborates these results, but provides additional information with important ramifications regarding the role *pdx-1* plays in posterior foregut development and organogenesis. First, the formation of the dorsal and ventral pancreatic buds apparently occurs normally in *pdx-1* homozygous null mutants. The ventral bud is not maintained as a discrete structure, while the dorsal bud undergoes limited branching outgrowth and forms a stunted, irregular epithelial tree that persists in newborn pups. Glucagon-expressing cells are detected in the mutant dorsal ductule, but immunohistochemical analysis of late gestation embryos fails to detect any insulin- or amylase-positive cells in this region. The current analyses do not preclude the transient existence of a population of insulin- or amylase-positive cells in earlier embryos, but we conclude that loss of *pdx-1* function prevents the differentiation of mature islets, acini, and β cells in perinatal embryos. Second, the architecture of the rostral-most duodenum is altered in perinatal *pdx-1*$^{-/-}$ embryos, such that it forms a contorted tube lined by a cuboidal (rather than columnar) epithelium that is continuous with the dorsal ductule and bile duct epithelium. Third, Brunner's glands fail to differentiate in homozygous null animals, and enteroendocrine cells are greatly reduced in number in the villus epithelium of the rostral duodenum.

pdx-1 expression in the embryonic gut

The pattern of β-gal expression derived from the pdx^{lacZko} allele agrees well with endogenous PDX-1 expression (Guz et al., 1995; Ohlsson et al., 1993; Miller et al., 1994; Leonard et al., 1993), but we report for the first time *pdx-1* expression in the antral stomach, common bile duct, and in the cystic and biliary ducts adjacent to the common bile duct. These data therefore expand the potential sphere of influence for *pdx-1* gene function in gut differentiation. Currently, we interpret the defects in *pdx-1* homozygous null mice as being restricted to the pancreas and rostral duodenum, but this view might well change if the other tissues could be scored for subtle differences in the expression of suitable markers.

By analyzing mice homozygous null for a Krox-20/β-gal fusion protein allele, Schneider-Maunoury et al. (1993) showed that the hindbrain rhombomeres normally expressing *Krox-20* were formed but subsequently degenerated in the absence of *Krox-20* function. Based on this paradigm, removing PDX-1 function could have caused the death of most or all endodermal cells normally expressing it. In contrast to this possibility, the persistence throughout development of PDX-1/β-gal-expressing cells in the rostral duodenum and pancreas in pdx$^{lacZko-/-}$ embryos indicates that these cells do not require *pdx-1* function for their survival, and that the establishment and maintenance of embryonic *pdx-1* expression boundaries does not involve an autoregulatory mechanism.

Posterior foregut patterning

At 8.5 dpc, the foregut pouch endoderm extends rostrally into the headfold, with its anteroventral surface in contact with precardiac mesoderm and the posterodorsal surface continuous with notochordal mesoderm. Starting at approximately 9.0 dpc, the pancreas and liver arise from bidirectional endodermal outgrowths of the posterior foregut. Most of the ventral outgrowth acquires a hepatic fate, with only the caudal-most portion forming the ventral pancreatic bud, while the dorsal outgrowth produces the dorsal pancreas. Previously, tissue recombination studies showed that precardiac mesoderm could induce hepatic endoderm (see for review Le Douarin, 1975), while axial mesoderm induced pancreatic endoderm (Wessells and Cohen, 1967). Therefore, posterior foregut regionalization could be considered to result from an interplay between opposing hepatic and pancreatic influences, with the endoderm becoming determined towards hepatic, pancreatic, or duodenal fates according to the relative strengths and overlap of the two programs. Of relevance to this concept of pancreatic/hepatic duality, pancreatic duct cells are able to regenerate mature pancreatic cell types (Shaw and Latimer, 1926), but destruction of pancreatic tissue by ethionine and regrowth in the presence of a mutagen results in the surprising appearance of hepatocytes (Scarpelli and Rao, 1981).

pdx-1 and pancreatic development

We hypothesize that a major component of the pancreatic development program is the localized induction by axial mesoderm of a specific endodermal *pdx-1* expression domain. The blocked proliferation and differentiation of pancreatic exocrine and endocrine cell types in *pdx-1*$^{-/-}$ animals, described here and by Jonsson et al. (1994), provides strong evidence consistent with this proposal. The accepted dogma for normal pancreatic development is that it results from a primary instructive induction of the endoderm by axial mesoderm, and secondary mesenchymal signals that induce outgrowth and branching morphogenesis. The latter signals are apparently noninstructive, since similar effects are produced by heterologous mesenchyme (Wessells and Cohen, 1967), and transfilter and protease experiments suggest that the signals are comprised of diffusible polypeptides (Golosow and Grobstein, 1962; Wessells and Cohen, 1967). The production of a dorsal pancreatic bud and its subsequent change in architecture to a branched epithelial outgrowth in *pdx-1*$^{-/-}$ embryos could represent a partial response to the mesodermal signals described above. However, without the specific developmental instructions provided by *pdx-1* expression, we propose that the pancreatic precursors cannot proliferate fully and do not differentiate into mature pancreatic cell types, as evidenced by the lack of amylase and insulin expression, and loss of normal tissue morphology. The analysis of the phenotype of *Hox11* homozygous null mutant mice (Roberts et al., 1994) suggests that a similar situation exists during development of the spleen, because the splenic precursors are generated normally, but then fail to differentiate and are lost through apoptosis (Dear et al., 1995).

We have presented data consistent with the notion that the dorsal ductule represents pre-pancreatic tissue arrested in an 'early embryonic' state. In *pdx-1*$^{-/-}$ embryos, the epithelium throughout the dorsal ductule remains GLUT2-positive at 16.5 dpc and 18.5 dpc, which contrasts the change in wild-type embryos from uniform GLUT2 expression in the buds to very low level expression in the mature pancreatic ducts. Notably, glucagon-expressing cells are present in the dorsal bud, and are still found later in the ductule derived from it, in *pdx-1*$^{-/-}$ animals (Figs 5 and 6). Together with the finding that many glucagon-positive cells in the 9.5 dpc bud do not express PDX-

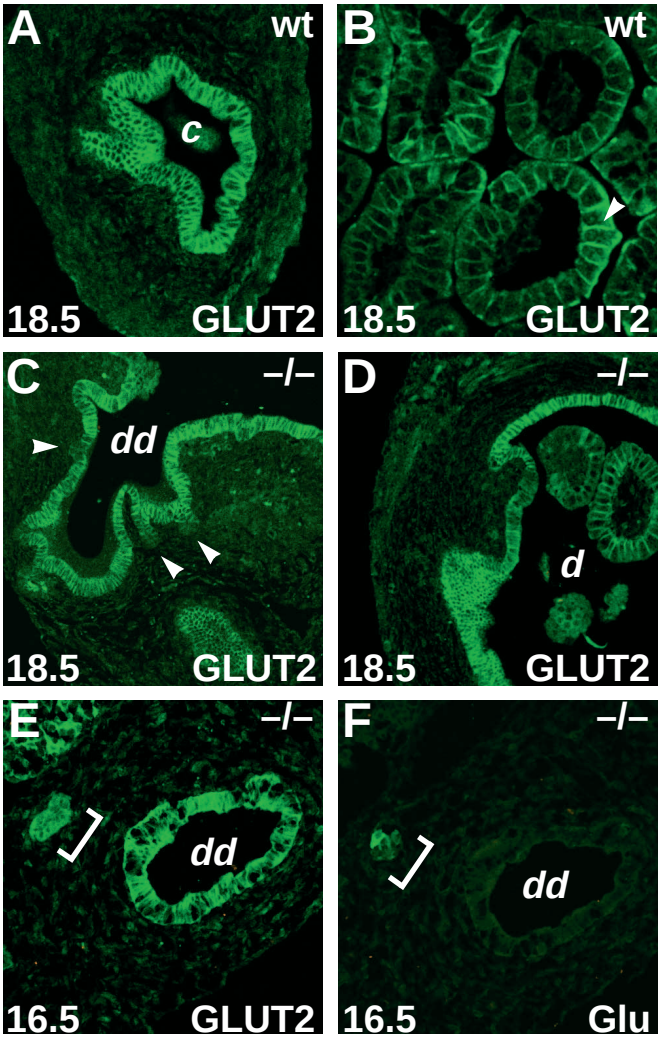

Fig. 6. GLUT2 expression in the dorsal ductule. The dorsal ductule and rostral duodenum were immunostained for insulin, glucagon, and GLUT2 expression at 16.5 and 18.5 dpc and imaged confocally. All sections were stained for insulin (assigned a red pseudocolor), and double-stained for glucagon (Glu) or GLUT2 (indicated in lower right corner, assigned green pseudocolor). Note that no insulin-positive cells are present in any panel. (A) High levels of GLUT2 are detected in the epithelial lining of the cystic duct (c) of $pdx^{lacZko+/-}$ embryos at 18.5 dpc. (B) However, GLUT2 signal in the villi of the same animals is found on the basolateral surfaces (arrowhead) of the columnar epithelium. (C) The dorsal ductule (dd) epithelium of –/– littermates has a cuboidal morphology similar to the cystic duct in A, and equally intense GLUT2 expression. Numerous evaginations of the ductule (arrowheads) show reduced GLUT2 signal. Note the continuation of intense GLUT2 signal into the aberrant cuboidal epithelium of the rostral-most duodenum (upper right region of C). (D) The GLUT2 signal in the abnormal duodenal epithelium is more intense than that in the villi (circular cross-sections within the lumen). Note that patches of reduced staining in the cuboidal epithelium correspond to regions of transition to normal columnar epithelium. (E,F) At both 16.5 dpc and 18.5 dpc (16.5 dpc shown), glucagon-positive cells are found at the tips of the GLUT2-positive evaginations of the dorsal ductule epithelium (white brackets), as well as within the epithelium proper (see Fig. 5I). c, cystic ducts; dd, dorsal ductule; d, duodenum; Glu, glucagon.

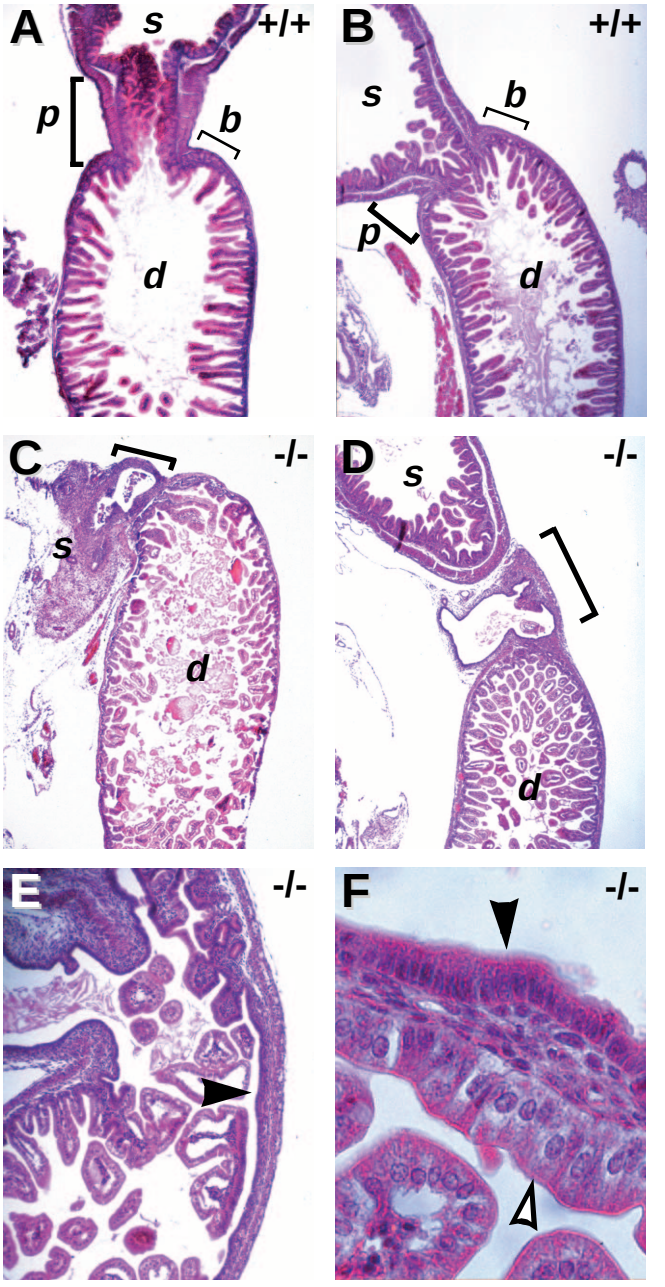

Fig. 7. Histological analysis of the stomach/duodenal region. The junction of the stomach and rostral duodenum was analyzed at 1 dpp and 18.5 dpc on serial sections by H&E staining. At 1 dpp (A) and 18.5 dpc (B), the stomach/duodenum junction of +/+ animals is well-defined with the pylorus (p) opening into the rostral duodenum. Brunner's glands (b) are found in a collar around the neck of the duodenum. This region of *pdx-1*$^{-/-}$ littermates at both stages (C, 1 dpp; D, 18.5 dpc) is malformed (unlabeled brackets). In most –/– animals, this region forms an undulated cavity lacking villi and lined by cuboidal epithelium that is continuous with the common bile duct and dorsal pancreatic ductule. (E) In a few –/– embryos, such a cavity is not present, but the abnormal smooth cuboidal epithelium (arrowhead) is clearly present. (F) Comparison at higher magnification of the cuboidal epithelium (black arrowhead) with normal villus columnar epithelium (open arrowhead) in the duodenum of $pdx^{XBko-/-}$ embryos, indicating the differences in morphology and H&E staining of the two epithelia. s, stomach; p, pylorus; d, duodenum; b, Brunner's glands.

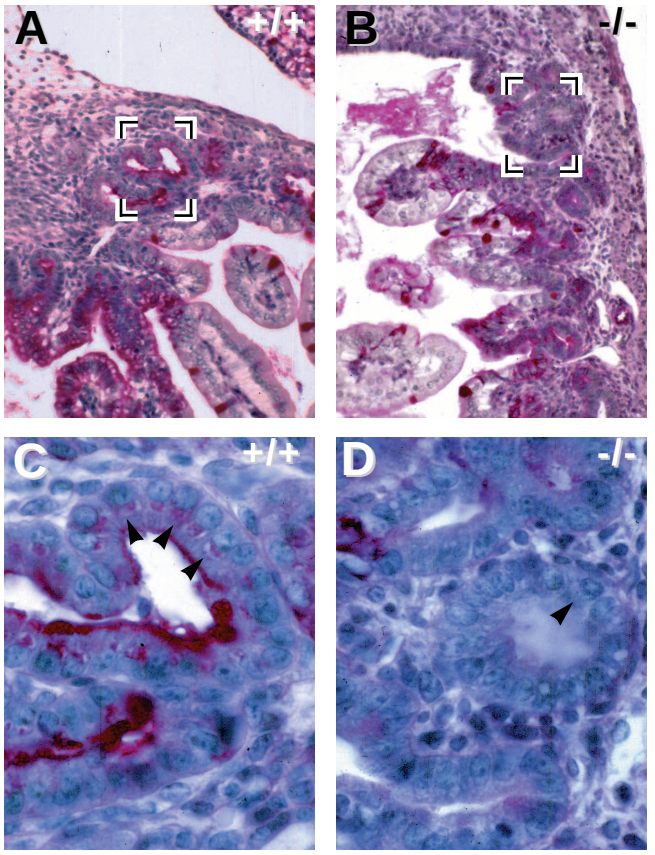

Fig. 8. Absence of Brunner's gland's in *pdx-1*$^{-/-}$ mutants. (A) In +/+ 18.5 dpc embryos, the Brunner's glands, located just below the pylorus (Fig. 7A), stain characteristically with PAS. (B) Circular structures morphologically resembling Brunner's glands are seen in some sections of –/– embryos. (C) High magnification of bracketed region in A shows PAS staining of the mucins on the lumenal surface and within the perinuclear Golgi (arrowheads) of Brunner's gland cells. (D) The indicated region of *pdx-1*$^{-/-}$ gut shown in B has a different morphology from that of Brunner's glands, and is PAS-negative (arrowhead indicates lack of perinuclear Golgi staining).

1/β-gal (Fig. 5A), this suggests that the induction of at least some putative islet α-cell precursors is independent of *pdx-1* function (Fig. 5B). However, a rigorous test of this possibility awaits the invention of methods for determining the lineage relationship of early 'pre-endocrine' cells to mature islet cells.

pdx-1 and duodenal development

The *pdx-1* gene is clearly required for normal rostral duodenal patterning, although it is not involved in the production of columnar epithelium, villi, and enteroendocrine cells *per se*, as they are all present in the more distal duodenum of *pdx-1*$^{-/-}$ animals, and outside the *pdx-1* expression domain. As described above, posterior foregut patterning may involve opposing hepatic and pancreatic programs. On this basis, we speculate that the mutant duodenum phenotype in *pdx-1*$^{-/-}$ animals could be explained by an expansion of 'hepatic influences' in the absence of *pdx-1* function, and that this results in the rostral-most duodenum adopting a bile duct-like fate. Consistent with this proposal, the cuboidal epithelium replacing the

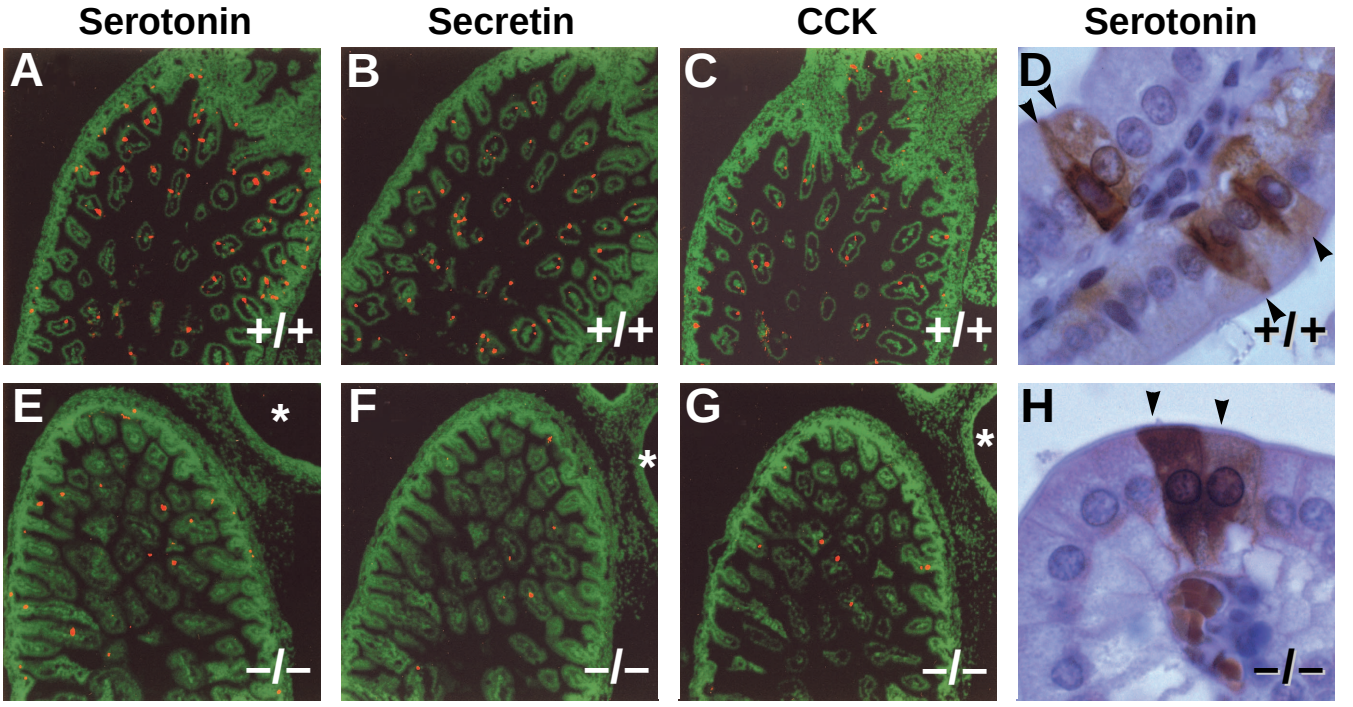

Fig. 9. Reduction in neuroendocrine cells in *pdx-1*$^{-/-}$ embryos. (A-C) Confocally imaged immunolocalization of enteroendocrine cells (red pseudocolor) shows abundant serotonin, secretin, and CCK-positive cells in the rostral-most duodenum of 18.5 dpc pdx$^{XBko+/+}$ animals. Nuclei were counterstained with YO-PRO-1 (green pseudocolor). (E-G) Similar analysis of pdx$^{XBko-/-}$ embryos reveals approx. 60% reduction in these neuroendocrine cells in the first 1 mm segment of columnar epithelium (see Fig. 10). The lumen of the aberrant cuboidal epithelium of the rostral-most duodenum is indicated (asterisks). (D,H) Immunoperoxidase detection in both +/+ and –/– embryos shows the characteristic morphology of these cells interspersed among the mucosal enterocytes (arrowheads indicate serotonin-positive cells).

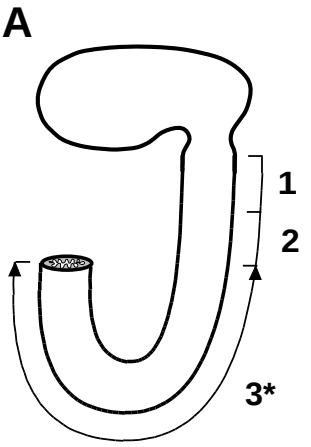

B

Reduction in Neurendocrine Cell-types within the Proximal Duodenum

Peptide	Segment	+/+	-/-	% normal
Serotonin	1	44 (+/-6.6)a	17 (+/-4.4)	38
	2	27 (+/-6.1)	16 (+/-2.9)	59
	3*	25 (+/-7.9)	23 (+/-4.4)	92
Secretin	1	33 (+/-9.3)	14 (+/-4.7)	42
	2	27 (+/-5.9)	13 (+/-3.8)	48
	3*	15 (+/-6.3)	14 (+/-3.3)	93
CCK	1	33 (+/-6.3)	11 (+/-4.0)	33
	2	22 (+/-2.2)	15 (+/-4.2)	68
	3*	19 (+/-4.3)	15 (+/-4.2)	79

Fig. 10. Quantitation of enteroendocrine cells in $pdx^{XBko-/-}$ embryos. (A) Neuroendocrine cells were counted over three 1 mm long segments of normal columnar epithelium in 18.5 dpc $pdx^{XBko+/+}$ and –/– embryos (four of each genotype). Segments 1 and 2 were adjacent, but differences in gut folding and sectional plane led to segment 3* often being separated from segment 2, as indicated by the double-headed arrow. In –/– embryos, segments 1 and 2 were displaced approx. 0.3 mm from the pylorus because of the abnormal cuboidal epithelium. For each segment (1,2,3) in all 8 embryos, markers were scored on four non-adjacent longitudinal sections, thus avoiding double-scoring of cells. (B) For each embryo analyzed, the average number of positive cells within segment 1, 2, or 3 was calculated. For each segment, the table shows the mean (± s.e.m.) of the four animals' individual averages. All three cell types show approx. 60% reduction in segment 1 of 18.5 dpc $pdx^{XBko-/-}$ animals, but their levels approach that of wild-type embryos in distal segments (e.g. serotonin).

villi lacks enterocyte-specific marker expression, and resembles the bile duct epithelium both in morphology and GLUT2 expression. The examination of other well-defined regional markers, once they become available, will be useful in addressing this idea more definitively.

Although the above hypothesis is attractive in many respects, we cannot rule out the possibility that the cuboidal epithelium in the rostral duodenum represents tissue arrested at an early, but probably abnormal, morphogenetic state. In this scenario, the pseudostratified gut epithelium undergoes the transition to a simple epithelial layer, but in the absence of *pdx-1* function cannot proceed to a more advanced architecture, and forms neither villi, enterocytes, nor enteroendocrine cells. However, it is currently unknown whether the normal development of the mouse gut ever includes a transient cuboidal epithelial state. Finally, it is possible that the absence of proper differentiation in the rostral duodenum and/or the absence of a directional pancreatic outgrowth simply results in a local disorganization, allowing the spread of a cuboidal epithelium, continuous with the biliary duct and dorsal ductule, into the rostral-most duodenum.

Just distal to the deformed rostral duodenum, superficially normal villi are formed, and enterocytes and most enteroendocrine cell types are produced. However, *pdx-1*$^{-/-}$ mutants still display defects in patterning of this region, as marked by a substantial suppression in the numbers of enteroendocrine cells. One explanation for this phenotype is that pdx-1 acts locally in the rostral duodenum, together with other factors, to affect directly the numbers of enterocyte versus enteroendocrine cells born from their common stem cells in the endodermal crypts. However, we cannot exclude the possibility that the under-production of enteroendocrine cells is indirectly caused by the defective development of the adjacent rostral-most duodenum and/or the blockage in pancreatic development.

In summary, the data presented here show that the initial generation and outgrowth of the pancreatic progenitors does not require *pdx-1* function. Their production therefore occurs via separate regulatory pathways upstream of *pdx-1*, by early endodermal programs in which *pdx-1* plays a redundant role, or they are directly induced by the adjacent mesoderm. Nonetheless, the data presented here strongly suggest that *pdx-1* is required for the proper differentiation program of the posterior foregut as a whole, including the duodenum, rather than affecting only pancreatic development.

We thank Laura Gamer for advice on embryo dissection and staining, and Linda Hargett for outstanding assistance in production and maintenance of mutant mouse lines. B. L. M. H. is an Investigator and P. A. L. is an Associate of the HHMI. This research was funded by NIH grants HD28062 (to C. V. E. W.) and DK42502 (to M. A. M. and C. V. E. W.), and the Howard Hughes Medical Institute.

REFERENCES

Bonnerot, C. and Nicolas, J. (1993). Application of *LacZ* gene fusions to postimplantation development. *Meth. Enz.* **225**, 451-469

Camper, S. A., Saunders, T. L., Katz, R. W. and Reeves, R. H. (1990). The *Pit-1* transcription factor gene is a candidate for the murine Snell dwarf mutation. *Genomics* **8**, 586-590.

Cohn, S., Simon, T., Roth, K., Birkenmeier, E., and Gordon, J. (1992). Use of transgenic mice to map *cis*-acting elements in the Intestinal Fatty Acid Binding Protein Gene (*Fabpi*) that control its cell lineage-specific and regional patterns of expression along the duodenal-colonic and crypt-villus axes of the gut epithelium. *J. Cell Biol.* **119**, 27-44.

Dear, T.N., Colledge, W.H., Carlton, M.B.L., Lavenir, I., Larson, T., Smith, A.J.H.., Warren, A.J., Evans, M.J., Sofroniew, M.V., and Rabbitts, T.H. (1995). The *Hox11* gene is essential for cell survival during spleen development. *Development* **121**, 2909-2915.

Fire, A., Harrison, S. W. and Dixon, D. (1990). A modular set of *lacZ* fusion vectors for studying gene expression in *Caenorhabditis elegans. Gene* **93**, 189-198.

Fitzpatrick, V. D., Percival-Smith, A., Ingles, C. J. and Krause, H. M. (1992). Homeodomain-independent activity of the fushi-tarazu polypeptide in *Drosophila* embryos. *Nature* **356**, 610-612.

Gehring, W. J., Qian, Y. Q., Billeter, M., Furukubo-Tokunaga, K., Schier, A. F., Resendez-Perez, D., Affolter, M., Otting, G. and Wuthrich, K. (1994). Homeodomain-DNA recognition. *Cell* **78**, 211-223.

Golosow, N. and Grobstein, C. (1962). Epitheliomesenchymal interaction in pancreatic morphogenesis. *Dev. Biol.* **4**, 242-255.

Guz, Y., Montminy, M. R., Stein, R., Leonard, J., Gamer, L. W., Wright, C. V. and Teitelman, G. (1995). Expression of murine *STF-1*, a putative insulin gene transcription factor, in beta cells of pancreas, duodenal epithelium, and pancreatic exocrine and endocrine progenitors during ontogeny. *Development* **121**, 11-18.

Hogan, B., Beddington, R., Costantini, F. And Lacy, E. (1994).

Manipulating the Mouse Embryo: A Laboratory Manual 2nd ed. Cold Spring Harbor, NY: Cold Spring Harbor Laboratory Press.

Jetton, T. L., Liang, Y., Pettipher, C. C., Zimmerman, E. C., Cox, F. G., Horvath, K., Matschinsky, F. M. And Magnuson, M. (1994). Analysis of upstream glucokinase promoter activity in transgenic mice and identification of glucokinase in rare neuroendocrine cells in the brain and gut. *J. Biol. Chem.* **269**, 3641-3654.

Jonsson. J., Carlsson, L., Edlund, T. and Edlund, H. (1994). Insulin-promoter-factor 1 is required for pancreas development in mice. *Nature* **371**, 606-609.

Krumlauf, R. (1994). Hox genes in vertebrate development. *Cell* **78**, 191-201.

Le Douarin, N. M. (1975). An experimental analysis of liver development. *Medical Biology* **53**, 427-455.

Leonard, J., Peers, B., Johnson, T., Ferreri, K., Lee, S. and Montminy, M. R. (1993). Characterization of somatostatin transactivating factor-1, a novel homeobox factor that stimulates somatostatin expression in pancreatic islet cells. *Mol. Endocrinol.* **7**, 1275-1283.

Li, S., Crenshaw, E. B. 3rd., Rawson, E. J., Simmons, D. M., Swanson, L. W. and Rosenfeld, M. G. (1990). Dwarf locus mutants lacking three pituitary cell types result from mutations in the POU-domain gene *pit-1*. *Nature* **347**, 528-533.

McGinnis, W. (1994). A century of homeosis, a decade of homeoboxes. *Genetics* **3**, 607-611.

Miller, C. P., McGehee, R. E. Jr. and Habener, J. F. (1994). IDX-1: a new homeodomain transcription factor expressed in rat pancreatic islets and duodenum that transactivates the somatostatin gene. *EMBO J.* **13**, 1145-1156.

Murphy, P. And Hill, R. E. (1991). Expression of the mouse *labial*-like homeobox-containing genes, *Hox 2.9* and *Hox 1.6*, during segmentation of the hindbrain. *Development* **111**, 61-74.

Ohlsson, H., Karlsson, K. and Edlund, T. (1993). IPF1, a homeodomain-containing transactivator of the insulin gene. *EMBO J.* **12**, 4251-4259.

Pang, K., Mukonoweshuro, C. and Wong, G. G. (1994). Beta cells arise from glucose transporter type 2 (Glut2)-expressing epithelial cells of the developing rat pancreas. *Proc. Natl. Acad. Sci. USA* **91**, 9559-9563.

Peers, B., Leonard, J., Sharma, S., Teitelman, G. and Montminy, M. R. (1994). Insulin expression in pancreatic islet cells relies on cooperative interactions between the helix loop helix factor E47 and the homeobox factor STF-1. *Mol. Endocrinol.* **8**, 1798-1806.

Peshavaria, M., Gamer L., Henderson, E., Teitelman, G., Wright, C. and Stein, R. (1994). XlHbox 8, an endoderm-specific *Xenopus* homeodomain protein, is closely related to a mammalian insulin gene transcription factor. *Mol. Endocrinol.* **8,** 806-816.

Roberts, C. W., Shutter, J. R. and Korsmeyer, S. J. (1994). *Hox11* controls the genesis of the spleen. *Nature* **368**, 747-749.

Roth, K. A., Rubin, D. C., Birkenmeier, E. H. and Gordon, J. I. (1991). Expression of liver fatty acid-binding protein/human growth hormone fusion genes within the enterocyte and enteroendocrine cell populations of fetal transgenic mice. *J. Biol. Chem.* **266**, 5949-5954.

Scarpelli, D. G. And Rao, M. S. (1981). Differentiation of regenerating pancreatic cells into hepatocyte like cells. *Proc. Natl. Acad. Sci. USA* **78**, 2577-2581.

Schneider-Maunoury, S., Topilko, P., Seitandou, T., Levi, G., Cohen-Tannoudji, M., Pournin, S., Babinet, C. and Charnay, P. (1993). Disruption of *Krox-20* results in alteration of rhombomeres 3 and 5 in the developing hindbrain. *Cell* **75**, 1199-1214.

Shaw, J. W. And Latimer, E. O. (1926). Regeneration of pancreatic tissue from the transplanted pancreatic duct in the dog. *Am. J. Physiol.* **76**, 49-53.

Solcia, E., Capella, C., Buffa, R., Usellini, L., Fiocca, R. and Sessa, F. (1987). Endocrine cells of the digestive system. In: *Physiology of the Gastrointestinal Tract*, 2nd ed. L. R. Johnson, ed. Raven Press, New York. pp 111-130.

Sweetser, E., Birkenmeier, E. H., Hoppe, P. C., McKeel, D. W., and Gordon, J. G. (1988). Mechanisms underlying generation of gradients in gene expression within the intestine: an analysis using transgenic mice containing fatty acid binding protein-human growth hormone fusion genes. *Genes Dev.* **2**, 1318-1332.

Teitelman, G., Alpert, S., Polak, J. M., Martinez, A. and Hanahan, D. (1993). Precursor cells of mouse endocrine pancreas coexpress insulin, glucagon and neuronal proteins tyrosine hydroxylase and neuropeptide Y, but not pancreatic polypeptide. *Development* **118**, 1031-1039.

Thorens, B., Cheng, Z., Brown, D. and Lodish, H. (1990). Liver glucose transporter: a basolateral protein in hepatocytes and intestine and kidney cells. *Am. J. Physiol.* **259**, C279-C285.

Wessells, N. K. and Cohen, J. H. (1967). Early pancreas organogenesis: morphogenesis, tissue interactions, and mass effects. *Dev. Biol.* **15**, 237-270.

Winnier, G., Blessing, M., Labosky, P. A. and Hogan, B. L. M. (1995). Bone morphogenetic protein-4 is required for mesoderm formation and patterning in the mouse. *Genes Dev.* **9**, 2105-2116.

Wright, C. V. E., Schnegelsberg, P. and De Robertis, E. M. (1988). *XlHbox 8*: a novel *Xenopus* homeo protein restricted to a narrow band of endoderm. *Development* **105**, 787-794.

(Accepted 11 December 1995)